Molecular Crystals and Liquid Crystals
Publication details, including instructions for authors and subscription information:
http://www.tandfonline.com/loi/gmcl18

Ferroelectric Liquid-Crystal Gray-Scale Response

David Armitage [a]

[a] Research & Development Division, Lockheed Missiles & Space Company, Inc., Palo Alto, CA, 94304

Version of record first published: 24 Sep 2006.

To cite this article: David Armitage (1991): Ferroelectric Liquid-Crystal Gray-Scale Response, Molecular Crystals and Liquid Crystals, 199:1, 97-110

To link to this article: http://dx.doi.org/10.1080/00268949108030921

Mol. Cryst. Liq. Cryst., 1991, Vol. 199, pp. 97–110
Reprints available directly from the publisher
Photocopying permitted by license only

Printed in the United States of America

Ferroelectric Liquid-Crystal Gray-Scale Response

DAVID ARMITAGE

Research & Development Division, Lockheed Missiles & Space Company, Inc., Palo Alto, CA 94304

(Received July 27, 1990)

The experimental behavior of a charge-controlled surface-stabilized ferroelectric liquid-crystal pixel of area 1 mm^2 is reported. Obliquely evaporated silicon-oxide alignment is compared with rubbed-nylon alignment. The experimental behavior of a distorted helix ferroelectric liquid-crystal cell is reported. Applications to optical correlator systems are discussed.

Keywords: ferroelectric LC, gray-scale

INTRODUCTION

Ferroelectric liquid crystals (FLC) are an emerging technology with advantages in bistability, speed, and contrast.[1] However, existing nematic liquid-crystal devices provide an analogue gray scale, necessary in TV display devices. The importance of gray scale is recognized in neural-net computing structures, and optical correlation favors ternary-state filters.[2,3] It is of interest to study FLC gray-scale behavior in relation to optical processing. There are several FLC mechanisms that can provide gray scale without sacrificing FLC speed advantage.

The surface-stabilized FLC (SSFLC) device structure provides bistability, which is essential for large-scale passive matrix addressing applications.[1] A bistable device is limited to black and white operation, but can provide gray scale via time or space multiplexing. In time multiplexing, the pixel on/off duration is adjusted to provide a given time-averaged gray level. Therefore, the effective frame time is proportional to the gray levels required; moreover, flicker effects are objectionable.

Space multiplexing provides gray levels through spatial averaging of subpixels. The frame speed and resolution are severely compromised when the subpixels are directly controlled by the addressing circuitry. However, subpixels can be created effectively within the SSFLC pixel by charge-control operating circuitry, with little compromise in speed and resolution.[1,4] The pixel area that can switch is controlled by the amount of charge that is fed to the pixel. Therefore, the gray scale is related to pixel control charge.

The bistable SSFLC configuration degenerates into a continuous gray-scale de-

vice above the FLC transition temperature. This soft-mode FLC (SMFLC) effect is associated with the close proximity of the FLC phase transition.[5] The SMFLC device behaves as a retardation plate with an electric-field controllable optic axis. The SMFLC device advantages are high speed (submicrosecond) and high contrast, but the higher voltage levels and temperature control required at this stage of development are a disadvantage.

The distorted helix ferroelectric (DHF) is an alternative FLC device configuration which provides gray scale.[6,7] The FLC used in this configuration must have a short helic pitch, smaller than the readout optical wavelength. Electric-field-induced distortions of the FLC helix then appear as an average change in birefringent axis direction. The electro-optic response is similar to the SMFLC, but the DHF mechanism differs. Low operating voltage (<2 V) is an important advantage of the DHF, but diffraction effects and limited contrast ratio appear to be a disadvantage at this stage of development. When the readout wavelength in the material is greater than FLC helical pitch the associated diffraction is suppressed. Therefore infrared laser diode sources have a further advantage in DHF optical processing applications, in addition to compactness.

We report some experimental studies of a SSFLC pixel operated under charge control to provide gray scale and DHF gray-scale effects. The device requirements in optical correlator systems are discussed.

OPTICAL CORRELATOR DEVICE REQUIREMENTS

The optical correlator has been developed for many years, but recent advances in hardware and filter design are extending the practical applications.[8] The standard correlator arrangement is shown in Figure 1, with an input spatial light modulator (SLM) providing the input scene, and a programmable filter SLM in the Fourier plane to provide shift-invariant discrimination. A bright spot appears in the output image plane, providing the position and correlation strength of the target defined by the filter program.[9] This is an example of two-dimensional optical processing,

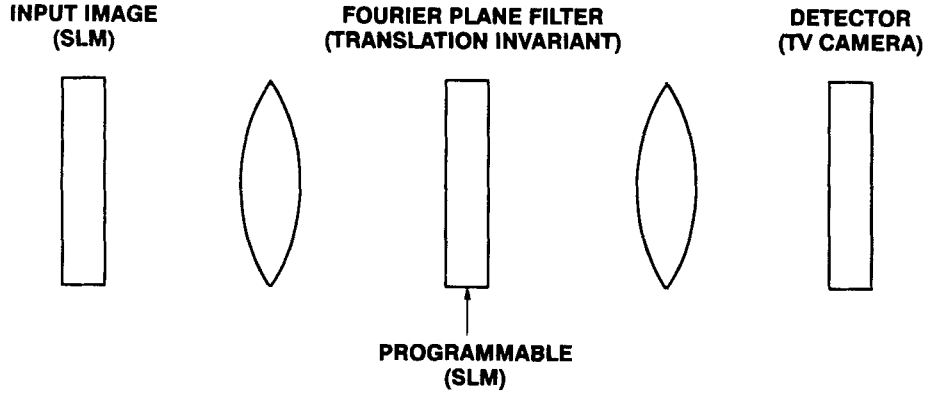

FIGURE 1 Optical correlator elements.

applicable to situations beyond the scope of digital electronics. The invention of the optical correlator preceded neural-net computing, but optical correlation can be described in neural-net language and can incorporate feedback.[10]

Binary amplitude modulation suffices at the correlator input, without significant loss of performance. The ideal filter represents the complex conjugate of the Fourier plane signal. Phase is the dominant aspect of coherent optics, and binary phase modulation suffices at the filter plane.[11] A more detailed study of performance shows the advantage of combined binary phase and binary amplitude, or ternary phase-amplitude filtering.[3] Further sophistication to a five-state filter can be justified.[12]

The dynamic range, efficiency, and resolution of liquid-crystal devices are appropriate to correlator requirements. The frame rate of the filter SLM, support electronics, and output detector array determines the correlation rate. The filter frame-rate demands are not expected to exceed 10 kHz, which can be achieved by FLC devices.

The optical complex amplitude (A_o) transmitted by a liquid-crystal cell positioned between orthogonal ideal polarizer and analyzer can be written

$$A_o = A_i \sin 2\theta H\{1 - \exp(-i\phi)\}/2 \tag{1}$$

where

A_i = input optical amplitude
ϕ = phase retardation of slow relative to fast axis
θ = optic axis rotation relative to the polarizer

The $\pm\theta$ rotations of the SSFLC about the polarizer direction provide the binary $\pm\pi/2$ phase modulation. The DHF provides similar binary $\pm\pi/2$ phase modulation, plus a zero-amplitude state at $\theta = 0$. The maximum output occurs at $\phi = \pi$. However, the binary phase condition relies on the constancy of ϕ and hence cell uniformity rather than absolute thickness. The output is also maximized by $\theta = \pi/4$, rather than $\theta = \pi/8$ for a display device.

Binary magneto-optical devices can provide the ternary phase-amplitude function, if the aperture of the system is restricted. A subpixel magnetic domain structure can then be induced, which diffracts light outside the aperture to give the required zero-amplitude state.[3] This approach is also valid for the SSFLC device and favors a small grain-domain structure.

Optical quality is a measure of wavefront distortion and should be better than 1/4 wave for coherent optic applications. Scattering and spurious diffraction effects should be avoided. The periodicity associated with pixelated devices gives rise to unwanted diffraction effects, but this can be mitigated by field fringing effects in the design of the liquid crystal SLM.[8]

CHARGE CONTROL GRAY SCALE

In the SSFLC device, the reversal of polarization (P_s) is associated with an optic axis rotation of 2θ in the bookshelf geometry, where θ is the intrinsic FLC smectic

C^* tilt or cone angle. If the input charge is restricted to $Q < 2P_s$, then only a fraction $Q/2P_s$ can switch before the applied electric field collapses. The fractional cell switching provides gray scale proportional to input charge.

There are a number of cell defects which can compromise the linearity and stability of the gray scale. Partial switching, where P_s is not precisely reversed and the optic axis rotates $<2\theta$, introduces nonlinearity and uncertainty in the relation between charge and average pixel brightness. The threshold voltage required for effective switching disturbs the linearity of the charge-control response. Surface-alignment forces favor a particular orientation and prevent long-term bistability. The electrical conductivity due to ionic impurities provides a discharge current which compromises the gray-scale response.

We are particularly interested in fast frame-rate devices driven by active matrix silicon addressing with reflective optical readout.[13,14] The gray scale must be established quickly ~100 μs, but memory beyond a refresh time of <10 ms is not important. The integrated silicon-addressing electronics requires ~100 μs to fully address one frame of a 512 × 512 array, so there is little advantage in a faster electro-optic response. High-quality optical-processing devices favor a precise alignment technology, e.g., obliquely evaporated silicon oxide. Double-pass, retro-reflective readout devices favor thin FLC layers approaching 1 μm.

FLC CELL FABRICATION

Charge-control SSFLC cells are fabricated from 3-mm-thick glass provided with transparent indium tin oxide (ITO) electrodes patterned as shown in Figure 2. The cell spacing is in the range of 1 to 2 μm, and the overlapping electrodes provide an active area of 1 mm^2. The small active area favors uniformity and reveals electrode-edge effects. The disadvantage is that stray capacitance must be minimized.

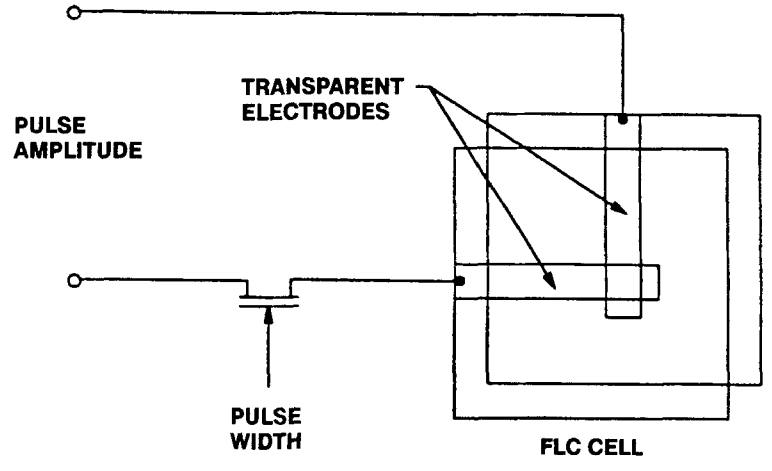

FIGURE 2 Cell electrode configuration with charge-control drive.

Liquid-crystal alignment is provided by e-beam evaporation of 50 nm of SiO_2 at a glancing angle to the substrate of 5 deg. Alternatively, the substrates are spin-coated with 1% solution of nylon 6/9 in formic acid, dried, then rubbed with rayon-velvet cloth. The substrates are assembled into cells with parallel rubbing, or evaporation directions, to promote minimum defects and maximum bistability. The cell substrates are cemented together with UV curing cement (Norland 61).

The FLC is capillary-flowed into the cells, under vacuum, at elevated temperature beyond the liquid-crystal clearing point, then slowly cooled to room temperature. The initial alignment and switching behavior of the cells are assessed, and the cell thickness is estimated by capacitance and optical measurements. The alignment uniformity of the nylon cells is improved by applying 50 V in the audio frequency range.[4,15] The SiO_2 cells are not improved by high-voltage treatment.

The DHF cells are assembled from similar, but unpatterned ITO substrates, providing a cell area of approximately 4 cm^2. The DHF performance favors alignment procedures which discourage bistable structures.[7] Evaporated oxide-alignment substrates are assembled into cells with antiparallel directions, since this is known to prevent bistability in SSFLC devices. However, the oxide-alignment layers have no influence on the orientation of DHF material FLC-6200 (F. Hoffmann-La Roche) used in all the DHF experiments.

DHF cells assembled from rubbed-nylon substrates impose the usual FLC alignment direction, but with poor uniformity. The uniformity is greatly improved by shearing the cell along the smectic plane direction, i.e., perpendicular to the cell rubbing direction. The cells fabricated for shearing have 6-μm-thick mylar-strip spacers.

The cell shear is performed by hand manipulation without the benefit of mechanical control devices. A switching voltage of ± 10 V at approximately 1 kHz, applied during the shearing operation, improves the uniformity. Oxide-alignment cells, lacking initial DHF orientation, are shear aligned with uniformity comparable to the nylon cells.

For the DHF interferometer experiment, cells are fabricated from 0.1 wave flat optical glass with ITO and antireflective coatings. Following shear alignment, the cells are fixed with cement.

SSFLC EXPERIMENTAL RESULTS

A voltage pulse is applied to the electrodes through a field-effect transistor in close proximity to the cells. The stray capacitance is of order 3 pF, which is small compared with the cell capacitance. The transister isolates the cell charge while the FLC switching process equilibriates. In repetitive switching it is necessary to return to a well-defined on or off state to avoid the accumulation of spurious responses.[4] The completely switched state is followed by a partially switched state, while zero average dc voltage is maintained through the applied voltage waveform shown in Figure 3.

The average transmission of the cell, between crossed polarizer and analyzer, is measured by a 633-nm HeNe laser beam illuminating the active cell area. The laser

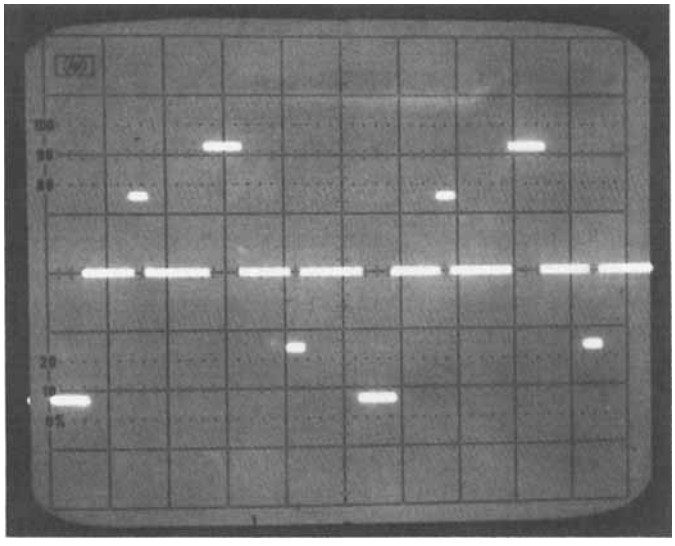

FIGURE 3 Cyclic switching waveform. Pulse position, duration, and repetition rates are controllable.

beam diameter is comparable to the active region of the cell. Figure 4 shows the typical response of FLC material ZLI3654 (E.M. Chemicals), which is approximately 1-μm thick. The reset pulses of amplitude ±12 V and 100-μs duration alternate the total dark and total bright states. The gray-scale levels are set by 2-μs pulses inserted between the reset pulses. The gray-scale transmission is independent of pulse length in the range 2 to 20 μs. A threshold voltage of ±0.5 V is observed for the oxide-aligned cell, while thresholds of +0.2 V and −2.1 V are associated with the nylon cell. The switching speed is alignment dependent, which is typical of SSFLC cells, being 400 μs (SiO_2) and 200 μs (nylon).

If the partially switched area of the cell is determined only by injected charge, then the response should be symmetrical about the reset levels. This is not the case, and all the cells show a lack of symmetry similar to Figure 4. The asymmetry is more pronounced in the strongly rubbed nylon-aligned cells, both in the gray-scale and threshold voltages.

Significant properties of FLC ZLI3654 are provided by the manufacture. At 20°C, spontaneous polarization P_s = 29 nC/cm^2; tilt angle θ = 25 deg; relative dielectric constants ε_1 = 5.5 and ε_{11} = 3.5 at 100 kHz; resistivity $\rho > 10$ GΩ.cm; and birefringence Δn = 0.13 at 600 nm.

The optic-axis switching rotation of the cells was measured as 48 deg (SiO_2) and 49 deg (nylon), which is slightly less than the 2θ = 50 deg for bookshelf alignment. The capacitance at 100 kHz of the two cells referred to in Figure 4 is measured at 46 pF (SiO_2) and 33 pF (nylon), implying cell thicknesses of 1.1 μm and 1.5 μm respectively. The on-state cell transmissions are consistent with these values. The dc resistances are 5 GΩ (SiO_2) and >10 GΩ (nylon), implying CR time constants >0.1 s.

The FLC polarization reversal in these cells requires a charge of 0.58 nC. This

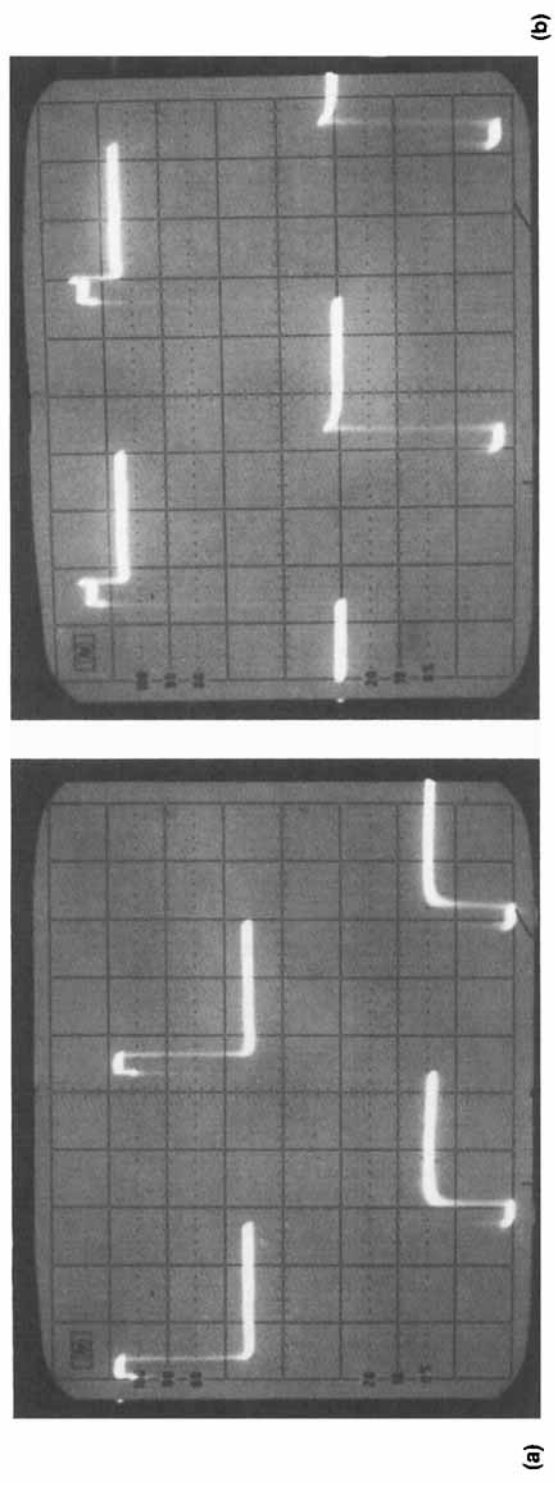

FIGURE 4 Optical transmission response to charge control cyclic switching waveform: ±12 V, 100-μs reset pulse, ±5-V, 2-μs gray-scale pulse. Horizontal timescale 5 ms/div. Linear vertical scale from zero to maximum transmission intensity. (a) silicon-oxide aligned cell; (b) nylon-aligned cell.

requires a short charging pulse voltage of 12.6 V and 17.5 V for SiO_2 and nylon, respectively. Lower voltages are required for pulse lengths comparable to the FLC switching time. The gray-scale switching voltage depends on voltage polarity, but if the voltage magnitudes are averaged, the 50% transmission level corresponds to a 7-V pulse, i.e., comparable to 50% of the full-charge maximum voltage level.

Polarizing microscope views of partially switched states are shown in Figure 5. The larger domain size in the SiO_2 cell is probably due to the more uniform alignment compared to the nylon cell. Gently rubbed nylon cells provide transmission characteristics similar to the SiO_2 aligned cells, but the domain structure shows considerably more disorder.

DHF EXPERIMENTAL RESULTS

The response of the DHF cell to a triangular voltage waveform of ± 4 V at 100 Hz and 1000 Hz is shown in Figure 6. The cell is placed between the crossed polarizer/analyzer and driven at 10 Hz while rotated to give a symmetrical transmission response to a 1-mm-diameter HeNe probe beam. At 100 Hz, a slight hysteresis is noticeable in the transmission intensity response. The hysteresis is marked at 1 kHz, where the maximum and minimum transmission values deteriorate. The cell thickness is not optimized for maximum transmission, but if polarizer losses are ignored, the maximum on-state transmission is 70%, with maximum on/off contrast ratio of 40.

The pulse voltage response is shown in Figure 7, where the cell is rotated to give equal, peak transmissions at ± 4-V, 5-ms pulses. The transmission is minimum during the 10-ms zero-voltage intervals. An expanded time scale shows a switch-

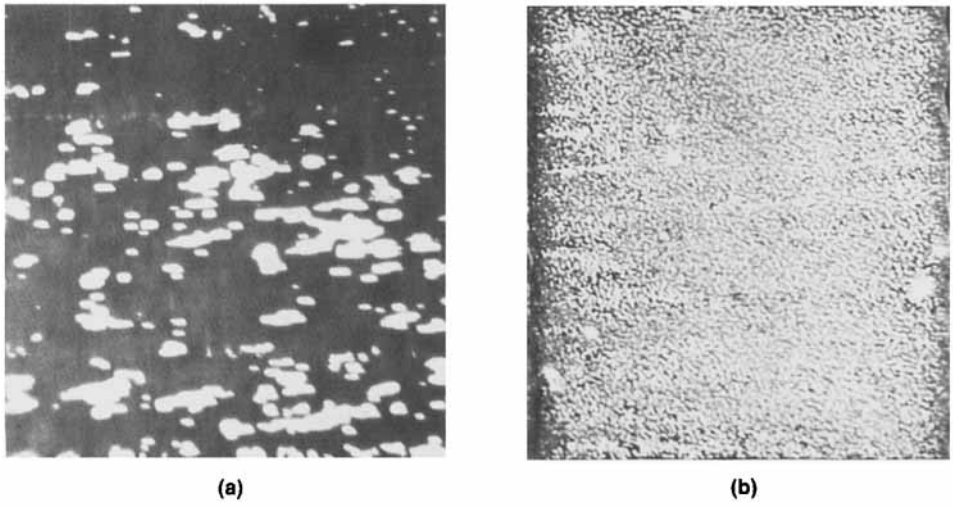

FIGURE 5 Polarizing microscope picture of partially switched gray-scale state of 1-mm² active area cell. (a) silicon-oxide aligned cell; (b) nylon-aligned cell.

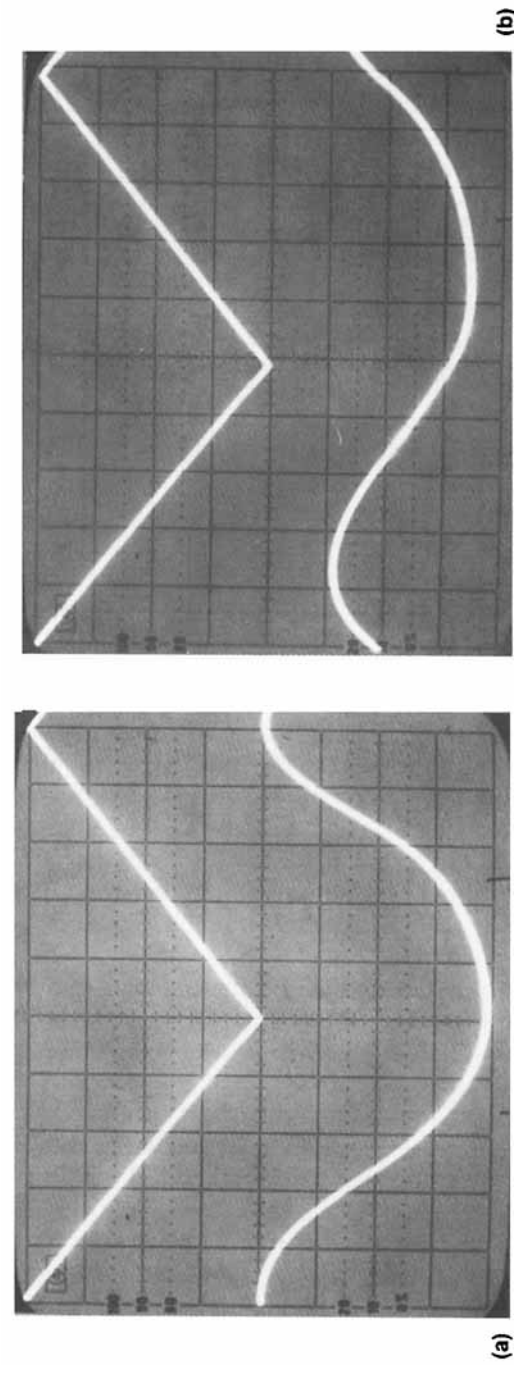

FIGURE 6 DHF device optical transmission intensity response to ± 4 V peak triangular waveform. (a) 100 Hz, (b) 1 kHz.

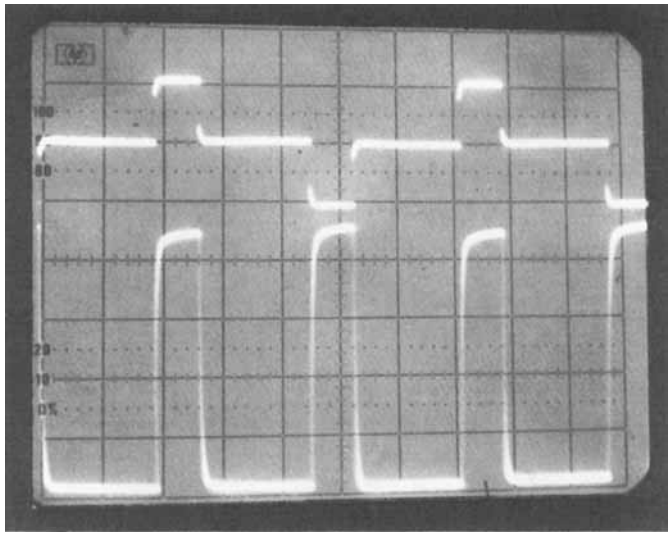

FIGURE 7 DHF device optical transmission intensity response to ±4 V, 5-ms pulses, with cell rotated for equal intensities and minimum transmission at zero voltage.

ing speed of order 100 μs. The optic axis rotations are measured at ±25 deg for ±4-V drive.

The response shown in Figure 7 is appropriate to a ternary phase-amplitude filter application.[3] The phase of the transmitted optical amplitude reverses with applied voltage polarity, while transmission approaches zero for zero voltage. Ignoring polarizer losses, the 25-deg optic axis rotation gives an optical throughput efficiency of 59%. The uniformity in the zero-voltage state is illustrated by the polarizing micrograph in Figure 8.

Increasing the voltage beyond ±4 V causes an increase in the off-state transmission, with no improvement in the on-state transmission. The higher voltages unwind the FLC helical structure, with consequent increase in zero-voltage relaxation time.

Some material characteristics of FLC 6200 are provided by the manufacturer: phase sequence of °C, Crystal-(-16)-Sx-(-3)-Sc*-(59)-Sa-64.5-isotropic; P_s = 100 nC/cm^2; switching time = 33 μs at 10 Vpp/μm; helical pitch = 370 nm; helix-unwinding field = 0.52 V/μm.

The helix-unwinding field implies a thickness of 8 μm for the cell reported here. This thickness is acceptable for a sheared 6-μm-mylar spaced cell. Scattering and diffraction effects are observed at the experimental 633-nm wavelength, but all the transmitted light is collected by a 1-cm^2-area photodiode close to the cell.

The zero-voltage helical periodicity is too short for diffraction at 633 nm, particularly when total internal reflection at the glass interface is considered. However, a diffraction line is always seen in a direction parallel to the nylon rub direction, which is orthogonal to the cell shear direction. This line vanishes with increasing voltage sufficient to unwind the FLC helix. In longer pitch FLC, close to the smectic-A transition, a diffraction line was reported which coalesces with decreasing tem-

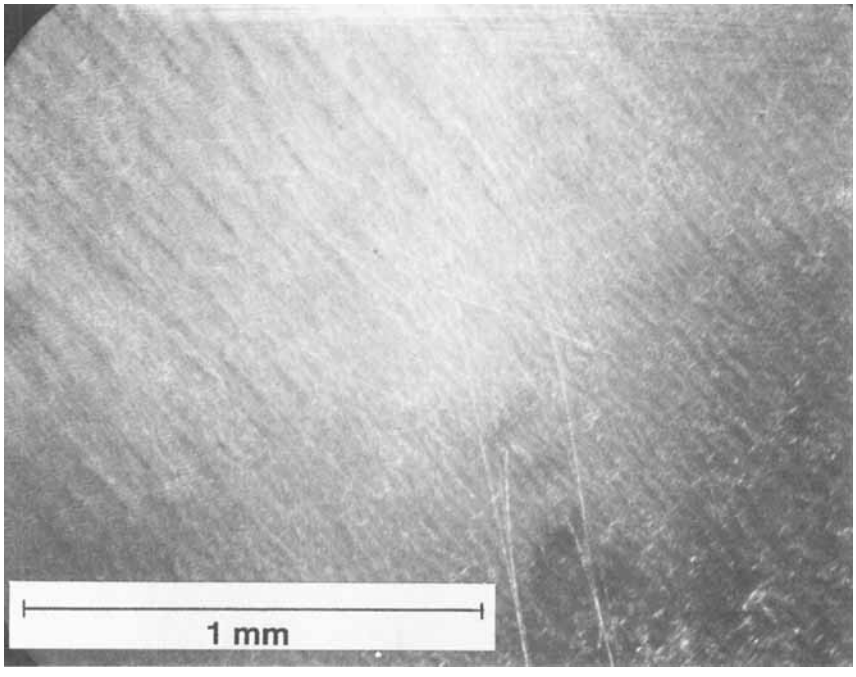

FIGURE 8 Polarizing microscope picture of DHF cell with zero applied voltage.

perature into diffraction spots appropriate to the helical periodicity.[16] The diffraction line was attributed to structural disorder in the initial formation of the chiral phase.

An additional diffraction line parallel to the shear direction is sometimes observed. The line is weak at low diffraction angles or spatial frequencies. The strength of this diffraction increases with unwinding voltage.

Binary phase modulation is demonstrated by the DHF cell fabricated from flat optical glass. The cell is operated in a Twyman-Green interferometer incorporating a polarizing beamsplitter, while the output is recorded on a video camera. Figure 9 illustrates a half-wave shift in the interference fringes between the $\pm\pi/2$ binary phase operating points. At zero cell voltage, the fringe visibility is poor, corresponding to the zero transmission state.

CONCLUSION

We have demonstrated a domain-switching gray-scale effect in SSFLC devices, that is similar to previous reports, but we extended the experiments to SiO_2 alignment.[4] The domain structure is sensitive to FLC alignment procedures. The gray level is related to the short-pulse charging level of the cell. Asymmetry in the switching response to alternate-charging polarities indicates that factors other than the charging pulse influence the gray level.

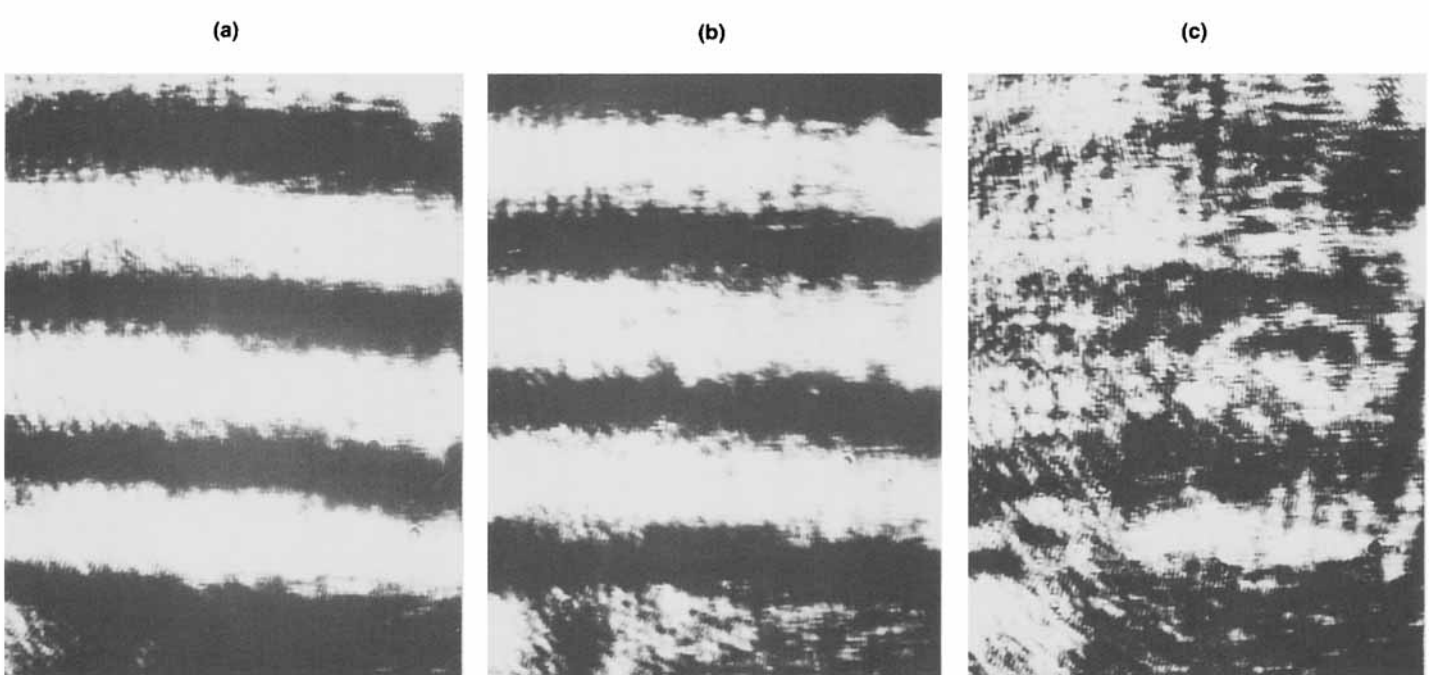

FIGURE 9 Interferometer fringes showing $\pm\pi/2$ binary phase modulation by DHF cell. (a) cell voltage +1 V, (b) −1 V, (c) 0 V. The fringes shift by half wave when the applied voltage is reversed.

Further work is required to determine the optimum cell structure for a given application. One polarity of the strongly rubbed nylon cell has the advantage of lower voltage requirement and low threshold, which could be of value in silicon integrated devices.[13] However, SiO_2 alignment is suitable for microcircuit applications, where rubbing alignment may be difficult to implement. Certain optical processing applications favor a small-grain domain structure, and this can be provided by appropriate surface treatment. Reliability and long-term stability need to be assessed.

The DHF results are consistent with earlier reports.[6,7] The difficulty of achieving uniform alignment in DHF devices poses an immediate problem. The alignment difficulty is associated with the absence of an alignment initiating nematic-like phase in FLC-6200. The situation is similar to the early days of SSFLC devices, when cell-shearing alignment processes were employed in device structures. Further development in DHF materials and alignment technology are anticipated, following the pattern of SSFLC device development. However, shear alignment could accommodate the small-scale production of optical processing devices.

The diffraction line orthogonal to the shear direction, which vanishes with the unwinding of the helical pitch, can be explained by disorder in the helical structure. The diffraction effects along the shear direction are also observed in SSFLC structures, and require further study.

We have demonstrated a ternary-state filter configuration using the DHF, capable of 59% throughput and 25:1 on/off contrast ratio. The contrast ratio is determined by alignment uniformity and should improve with further development.

We have fabricated a silicon circuit back plane, reflective readout, 12 × 12 array to test the gray-scale behavior in a realistic device environment. Each of the 144 pixels is driven by an integrated FET controlled by off-chip addressing circuitry. Off-chip addressing allows flexibility in experimental gray scale drive waveforms. Preliminary results on the response of this device with DHF readout are reported elsewhere.[14]

Acknowledgment

The assistance of Steve Ichiki (photolithography and e-beam deposition), Angie Ortega (photolithography), and Mike Wagner and Ernie Trujillo (electronics) is appreciated. Technical discussion with Mark Handschy (Displaytech Inc.) is acknowledged. We are grateful for a sample of FLC-6200 from Martin Schadt (F. Hoffman-La Roche). The work is supported by a Lockheed Research & Development Division program.

References

1. S. T. Lagerwall, N. A. Clark, J. Dijon and J. F. Clerc, *Ferroelectrics*, **94**, 3 (1989).
2. A. Von Lehmen, E. G. Paek, P. F. Liao, A. Marrakchi and J. S. Patel, *Opt. Lett.*, **14**, 928 (1989).
3. B. A. Kast, M. K. Giles, S. D. Lindell and D. L. Flannery, *App. Opt.*, **28**, 1044 (1989).
4. W. J. A. M. Hartmann, *J. App. Phys.*, **66**, 1132 (1989).
5. G. Andersson, I. Dahl, L. Komitov, S. T. Lagerwall K. Skarp and B. Stebler, *J. App. Phys.*, **66**, 4983 (1989).
6. L. A. Beresnev, V. G. Chigrinov, D. I. Dergachev, E. P. Poshidaev, J. Funfschilling and M. Schadt, *Liq. Cryst.*, **5**, 1171 (1989).

7. J. Funfschilling and M. Schadt, *J. App. Phys.*, **66**, 3877 (1989).
8. E. R. Washwell, R. Geblein, G. Gheen, D. Armitage and M. A. Handschy, *SPIE Proc.*, **1297**, 64 (1990).
9. N. Collings, "Optical Pattern Recognition Using Holographic Techniques," Addison-Wesley, UK, 1988.
10. H. J. Caulfield and D. Armitage, *App. Opt.*, **28**, 4060 (1989).
11. J. L. Horner and H. O. Bartelt, *App. Opt.*, **24**, 2889 (1985).
12. B. V. K. V. Kumar and J. M. Connelly, *SPIE Proc.*, **1151**, 166 (1989).
13. L. K. Cotter, T. J. Drabik, R. J. Dillon and M. A. Handschy, *Opt. Lett.*, **15**, 291 (1990).
14. D. Armitage and D. K. Kinnel, *SPIE Proc.*, **1296**, 158 (1990).
15. J. S. Patel, Sin-Doo Lee and J. W. Goodby, *Phys. Rev.*, **A40**, 2854 (1989).
16. K. Kondo, H. Takezoe, A. Fukuda and E. Kuze, *J. Appl. Phys.*, **21**, 224 (1982).